Design and Optimization Methodology for Permanent Magnet Synchronous Machines for Automotive Applications

Vinicius Vieira Ferreira
Matheus Henrique Rodrigues Miranda
Ludmila Corrêa de Alkmin e Silva
Integrated Systems Laboratory, School of Mechanical Engineering – Universidade Estadual de Campinas- UNICAMP, Brazil

ABSTRACT

Permanent Magnet Synchronous Motors (PMSMs) are gaining visibility in the automotive industry due to their high efficiency, power, and torque compared to other alternatives, such as Induction Motors. PMSMs also cover a wide range of speeds, making them especially suitable for applications in electric and hybrid vehicles. Their structure consists of using permanent magnets in the rotor, which generate electromagnetic torque from the alignment between the magnets and the phases of the stator. In this context, this study aims to review fundamental methodologies for sizing, analyzing, and optimizing the geometry of PMSMs. Therefore, a comprehensive literature review will be carried out, encompassing the main topologies and characteristics of electric motors used in the industry. Additionally, a technique for determining the optimal sizing, performing analysis, and optimizing the geometry of the motor based on electromagnetic scaling laws will be explored in detail. As a result, an overview comprising the main steps in the development of PMSM projects will be defined. This overview will be crucial to conduct the project for applications in different contexts. Therefore, this research aims to provide an overview of PMSMs, their sizing, analysis, and optimization of their geometry.

Keywords: Permanent magnet synchronous machines, design, analysis, scaling laws.

INTRODUCTION

Climate change is one of the greatest challenges humanity faces today. These changes are a direct result of the negative impacts caused by environmental degradation and high greenhouse gas emissions in recent years (Celik, 2020). In this context, Brazil and other countries are committed to pursuing sustainable pathways.

One of the sectors under the most pressure to adapt is the automotive industry, which faces growing demands to develop vehicle technologies capable of significantly reducing pollutant emissions and minimizing environmental impact (Miller, 2017). This is especially relevant, given that road transport is one of the main contributors to air pollution (Huang, 2021). A widely discussed alternative to address this challenge is vehicle electrification and hybridization, achieved through the adoption of fully electric or hybrid vehicles, which combine internal combustion engines with electric motors.

In this context, there is a need to study electric motor (EM) topologies to optimize aspects such as energy efficiency and material usage. Various topologies are used in the industry, depending on desired characteristics and specific applications. Among the most common electric motor topologies are synchronous (with or without permanent magnets) and asynchronous motors. Permanent Magnet Synchronous Motors (PMSMs) are a widely used topology, showing significant market growth (De Bem, 2021). These motors offer high efficiency and power density due to the use of permanent magnets with high remnant magnetic flux density (Br).

However, the efficiency and performance of PMSMs depend on proper motor sizing, which includes geometric parameters (rotor and stator), winding design, permanent magnet arrangement, and material selection. Thus, developing an electric motor design methodology is necessary to optimize performance.

This study conducts a literature review on the operating principles, topologies, and design methodologies of PMSMs, focusing on automotive applications. The fundamental characteristics of these motors are detailed, identifying key parameters for analysis and sizing. A scaling law-based EM sizing methodology is then presented, allowing the evaluation of a similar motor's performance based on a reference motor using scaling factors and analytical relationships.

After analyzing and simulating the reference and scaled motors using Finite Element Method (FEM) software, comparisons are made between the scaled motor's parameters obtained through scaling laws and FEM. Scaling laws can yield parameters close to those obtained via FEM, as demonstrated in (scaling laws) and (ultra-fast scaling laws). Thus, the proposed PMSM sizing methodology based on a reference motor can significantly reduce design and analysis time, especially in early project stages and geometry optimization for a given objective,

such as torque-speed-efficiency curve sizing (Zuluaga, 2021).

OPERATING PRINCIPLE OF AN ELECTRIC MOTOR

Electric machines are devices capable of converting energy between mechanical and electrical forms, operating either as motors or generators (Hanselman, 2006). They are called motors when converting electrical energy into mechanical energy and generators when performing the reverse conversion (Hanselman, 2006). In rotating electric machines, these conversions occur through the interaction between the magnetic field of a stationary part (stator), produced by alternating electrical excitation in conductors, and the magnetic field of a moving part (rotor), generated either by electrical excitation in a conductor or by permanent magnets (Ruwer, 2015). There are also electric machines that operate on the reluctance principle, without excitation or permanent magnets, as will be discussed later.

d-q Reference Frame

The Clarke-Park transformation, also known as dq0, is a fundamental mathematical tool for analyzing and controlling three-phase electric machines (Hanselman, 2006). This transformation converts variables from the three-phase abc reference frame (voltages, currents, inductances, etc.) into an orthogonal dq0 frame with "direct" (*d*) and "quadrature" (*q*) axes, applicable in both the stationary stator reference frame (DQ) and the rotating rotor reference frame (dq) (Hanselman, 2006). The *d*-axis represents the magnitude of electrical quantities aligned with phase *a*, while the *q*-axis is orthogonal to the *d*-axis in electrical angles (Pyrhonen et al., 2014). Thus, a variable F from the stationary ABC frame can be expressed in the DQ frame, as shown in Figure 1 and Equations 1 and 2 (Liu, 2013). From these, the *d* and *q* components in the rotating frame are derived using the supply frequency (*ω_e = poles/2*) or the rotor mechanical speed (ω_r), as illustrated in Figure 2 and Equations 3 and 4 (Liu, 2013).

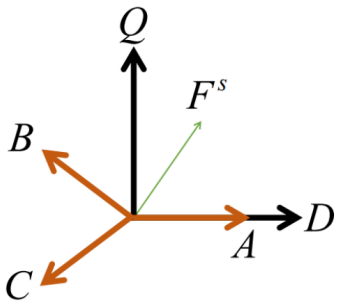

Figure 1: Three-phase stationary reference frame *ABC* and stator reference frame *DQ*. Source: Author.

$$F_D = \frac{2}{3}\left(F_A(t) - 0,5\,F_B(t) - 0,5\,F_C(t)\right) \quad (1)$$

$$F_Q = \frac{1}{\sqrt{(3)}}\left(F_B(t) - F_C(t)\right) \quad (2)$$

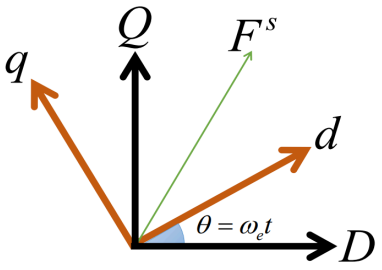

Figure 2: Stationary DQ and rotational d-q reference frames. Source: Author.

$$F_d = F_D\,cos(\omega_e t) + F_Q\,sin(\omega_e t) \quad (3)$$

$$F_q = -F_D\,sin(\omega_e t) + F_Q\,coe(\omega_e t) \quad (4)$$

The main advantage of this transformation is the conversion of time-varying sinusoidal quantities into direct current (DC) quantities, significantly simplifying the analysis and control of electric machines. This also facilitates system sizing and optimization, particularly in applications like PMSMs, where precise torque and speed control are essential (Zuluaga, 2021).

Key Analysis Parameters

For electric motor analysis, especially PMSMs, certain characteristics and parameters are critical for evaluating performance. These include:

- Number of poles and slots;
- Power, current, and voltage;
- Inductances and flux linkages in the **d-q** reference frame;
- Magnetic flux density distribution.

Alignment and Reluctance Torque

The electromagnetic torque produced by an electric motor can be derived from Equation 5 (Pyrhonen et al., 2014). The first component of the equation - $\frac{3}{2}\frac{p}{2}(L_d - L_q)i_d i_q$ - corresponds to reluctance torque, generated by the difference between the *d*-axis and *q*-axis inductances (Ruwer, 2015). Reluctance interactions arise from alignment forces between the stator's magnetic flux and rotor regions with lower magnetic reluctance, producing torque (Ruwer, 2015).

The second term - $\frac{3}{2}\frac{p}{2}\Psi_{PM} i_q$ - represents alignment torque, produced by the interaction between the

permanent magnet (PM) flux and the stator winding flux in the q-axis, which can be understood as an equilibrium point (Pyrhonen et al., 2014). During motor operation, this equilibrium shifts between coils at the supply frequency, generating alignment torque (Ruwer, 2015).

$$T_e = \frac{3}{2}\frac{p}{2}(L_d - L_q)i_d i_q + \frac{3}{2}\frac{p}{2}\Psi_{PM} i_q \quad (5)$$

TOPOLOGIES OF ELECTRIC MOTORS

According to Hanselman (2006), electric motors can be classified by their power supply type: direct current (DC) or alternating current (AC).

DC Motors

DC motors are used in applications requiring precise speed/torque control, rapid acceleration, and low power ranges but are unsuitable for automotive propulsion (Pyrhonen et al., 2014). Their key limitation lies in the use of mechanical commutators and brushes, which sequentially energize motor phases (a process called commutation) and require frequent maintenance due to brush wear (Hanselman, 2006; Pyrhonen et al., 2014).

AC Motors

AC motors eliminate brushes and commutators, relying instead on electronic devices to control phase switching and rotational speed (Hanselman, 2006). This study focuses on AC motors.

Asynchronous Motors

AC motors can be synchronous or asynchronous (i.e., whether rotor speed is synchronized to the supply frequency). A common asynchronous example is the squirrel-cage induction motor, widely used in industrial and automotive applications. Here, the stator's magnetic flux induces a rotor current in the conductive bars at a slightly lower speed, producing torque through slip—the speed difference between stator and rotor fields (Hanselman, 2006). Slip generates rotor currents, which interact with the stator's airgap flux to produce torque (Pyrhonen et al., 2014).

Low-voltage induction motors (50–1000 V) deliver 0.18–710 kW, with optimal voltage-power combinations (Pyrhonen et al., 2014). However, rotor I^2R losses reduce efficiency, and speed control is challenging in high-precision applications due to conductor resistance variations (Hendershot, 1994).

Synchronous Motors

In synchronous motors, rotor speed synchronizes with the stator's supply frequency. Common types include (Pyrhonen et al., 2014): (1) Separately Excited Synchronous Motors (SSM): Use DC-fed rotor windings instead of permanent magnets; (2) Synchronous Reluctance Motors (SyRM): Rely solely on reluctance torque by maximizing L_d - L_q differences and (3) Permanent Magnet Synchronous Motors (PMSM): The focus of this study.

PMSM Subtypes

Axial-Flux PMSMs feature dual stators and a central rotor, balancing magnetic forces for higher torque density (Hanselman, 2006). Used in space-constrained applications. Radial-Flux PMSMs are dominant in automotive applications. Two rotor designs exist: Surface-mounted PMSMs (SPMSM), in which magnets are mounted to the rotor surface. Only alignment torque is produced, and it is prone to mechanical stresses at high speeds; Interior PMSMs (IPMSM), in which embedded magnets create $L_q > L_d$ enabling both alignment and reluctance torque. More robust, efficient at high speeds, and reduce rare-earth magnet usage (Zuluaga, 2021).

A permanent Magnet-Assisted SynRM (PMaSyRM): Combines SyRM and IPMSM advantages, minimizing rare-earth dependency—a key trend due to cost/geopolitical factors (Zuluaga, 2021). This is the topology studied here.

SCALING LAW FOR ELECTRIC MOTORS

Scaling laws (or similarity laws) are used in various fields of physics and engineering, such as correlations between small- and large-scale models, thermodynamic correlations, etc. They are used to predict a design's performance based on data from an existing design (Stipetic et al., 2016). In electromagnetic applications, two models may have similar geometries but different materials and excitations. Stipetic and Zarko (2016) comprehensively defined scaling laws for PMSMs, which include radial, axial, and winding (rewinding) scaling, where the saturation levels of both models are preserved, enabling quick and accurate parameter estimation for the scaled model. Using these three scaling methods, they can be applied to any PMSM based on length, diameter, or voltage constraints, or performance requirements such as torque, power, efficiency, etc. (Stipetic et al., 2016).

For scaling laws to be valid, the magnetic fields of the reference motor and scaled motor must be identical (the magnetic flux density remains unchanged between the two models). Additionally, the geometries must be similar, and the materials, technologies (winding type, fill factor, etc.), and operating temperature must be the same (Stipetic & Zarko, 2015). Mechanical losses and permanent magnet losses will be neglected. In the following relationships, parameters with subscript 0 refer to the reference motor parameters.

Rewinding

Rewinding, or winding scaling, is used to adapt the motor winding for the power supply system's nominal

voltage or current (Stipetic Zarko, 2015) by changing the number of conductor turns per coil (N□) and the number of parallel conductors (a□) through a winding factor k_v (Equation 6), while maintaining the same geometry, produced electromagnetic torque, and current density *J*.

$$kW = \frac{Nc}{ap} \quad (6)$$

In rewinding, the maximum number of parallel conductors (a□) is determined by the reference motor's magnetic symmetry, being equal to the periodicity (greatest common divisor of the number of slots and poles) (Stipetic et al., 2016). For the number of conductor turns per coil, there is a manufacturing limitation related to changes in the copper fill factor in the slots or due to the conductor dimensions used (Stipetic et al., 2016).

Axial scaling

Axial scaling is the change in length l of the laminations and permanent magnets by a factor kA, while maintaining the same cross-sectional geometry of the reference motor (Equation 7) (Stipetic et al., 2016).

$$kA = \frac{l}{l_0} \quad (7)$$

Radial scaling

Radial scaling is the change in x and y dimensions of the reference motor's cross-section by a factor kR (Stipetic, Darko, 2015). In this procedure, magnetic flux densities B are preserved, and current density J is modified (Equation 9) (Stipetic et al., 2016).

SCALING LAW ALGORITHM

A scaling law application algorithm is presented by Stipetic et al. (2016), suggesting the order of applying scaling factors to the reference motor. Initially, axial and radial scaling should be performed, as these procedures modify the motor's torque and supply voltage, followed by rewinding for the available power supply. The algorithm proposed by Stipetic et al. (2016) begins with axial scaling to achieve the required torque for the scaled motor, since the scaling relationships for produced electromagnetic torque are volumetric and independent of other performance parameters (Equation 10) (Stipetic et al., 2016). For this purpose, maximum and minimum values for lamination length l are used, considering manufacturing limitations (Stipetic et al., 2016).

The equations for obtaining important analysis parameters of the scaled motor from the reference motor are presented by Stipetic et al. (2016), using the three scaling factors (kA, kR, and kW). Below are the scaling relationships for parameters with subscript 0 referring to reference motor parameters, neglecting end-winding influences (Equations 8-26).

$$I_{d/q} = \frac{k_R}{k_W} I_{d0/q0} \quad (8)$$

$$J = \frac{1}{k_W} J_0 \quad (9)$$

$$T_{em/shaft} = k_R^{\,2} k_A T_{em0/shaft0} \quad (10)$$

$$P_{em/shaft} = k_R^{\,2} k_A P_{em0/shaft0} \quad (11)$$

$$P_{Cu} = k_A P_{Cu0} \quad (12)$$

$$P_{in} = k_R^{\,2} k_A \left(P_{em0} + \frac{1}{k_R^{\,2}} P_{Cu0}\right) \quad (13)$$

$$P_{Fe} = k_R^{\,2} k_A P_{Fe0} \quad (14)$$

$$D = k_R D_0 \quad (15)$$

$$h_s = k_R h_{s0} \quad (16)$$

$$b_s = k_R b_{s0} \quad (17)$$

$$A_{slot} = A_{slot0} k_R^{\,2} \quad (18)$$

$$l_{stk} = k_A l_{stk0} \quad (19)$$

$$L_{d/q} = k_W^{\,2} k_A L_{d0/q0} \quad (20)$$

$$R_{ph} = \frac{k_W^{\,2}}{k_R^{\,2}} k_A R_{ph0} \quad (21)$$

$$V_{ph} = k_W k_R k_A V_{ph0} \quad (22)$$

$$V_d = k_W\left[\frac{k_A}{k_R} R_{ph0} I_{d0} - k_R k_A \omega_0 \psi_{magq0} - \omega_0 k_R k_A (L_{q0} I_{q0} + L_{dq0} I_{d0})\right] \quad (23)$$

$$V_q = k_W\left[\frac{k_A}{k_R} R_{ph0} I_{q0} + k_R k_A \omega_0 \psi_{magd0} + \omega_0 k_R k_A (L_{d0} I_{d0} + L_{dq0} I_{q0})\right] \quad (24)$$

$$PF = \frac{V_d I_d + V_q I_q}{VI} \quad (25)$$

$$eff = \frac{P_{shaft0}}{P_{em0} + \frac{1}{k_R^{\,2}} P_{Cu0}} \quad (26)$$

Design methodology using scaling laws

The electromagnetic design methodology for PMaSyRMs in this study follows three main stages: (1) Reference motor analysis using the Finite Element Method (FEM) and acquisition of key motor parameters, (2) determination of scaling factors (kA, kR and kW) based on requirements for the scaled motor, and (3) application of scaling laws to obtain key analysis parameters for the scaled motor. The scaled motor is also analyzed using FEM in Ansys Electronics Workbench software with the Maxwell 2D tool.

In this study, the 2004 Toyota Prius hybrid electric motor was used as the reference motor due to the abundance of available studies about its characteristics and performance in references such as [13], [14] and [15]. Using parameters from these references, the motor was modeled in FEM software (Figure 3) to analyze and verify important parameters for scaling relationships, as well as motor characteristics such as magnetic flux density distribution.

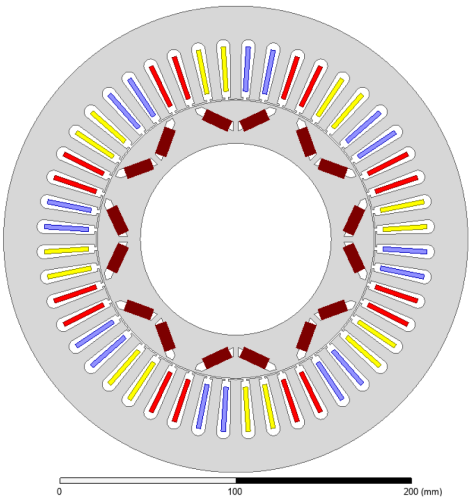

Figure 3: Referent motor built in FEM software (*Toyota Prius* 2004). Source: Author.

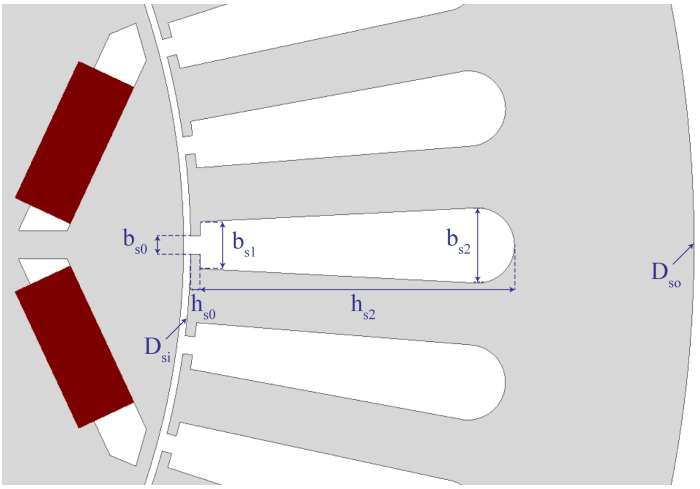

Figure 4: Geometric parameters of the stator. Source: Author.

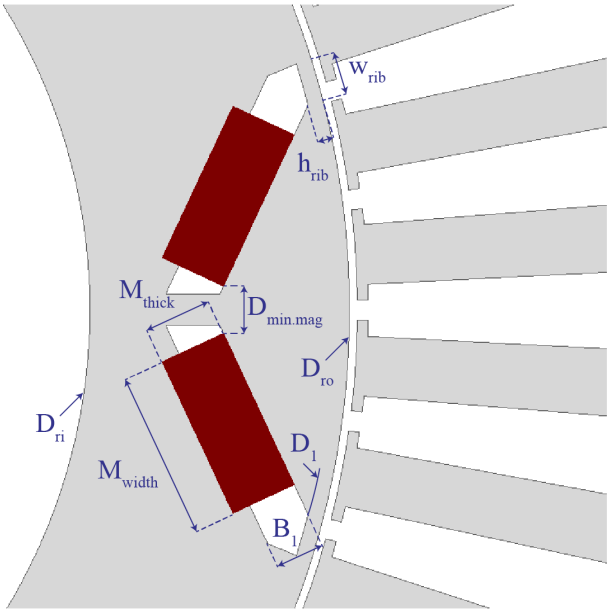

Figure 5: Geometric parameters of the rotor and permanent magnets. Source: Author.

For the new application, as an example, axial and radial scaling factors (kA and kR) of 0.5 were used, which when rewound for the same reference motor voltage (VLL0), resulted in kW equal to 0.125. From the scaling relationships (Stipetic et al., 2016), it is then possible to obtain important reference motor analysis parameters to evaluate its performance.

With the scaling law equations defined and presented, MATLAB software was used to implement the scaling routine. Subsequently, with both scaled and reference geometries obtained, virtual models of these electrical machines were built in FEM software. Figures 4 and 5 detail the geometric parameters of the stator, rotor and permanent magnets.

RESULTS AND DISCUSSION

The scaled motor is then modeled in FEM software to obtain its parameters (FEM scaled) and compare with parameters obtained through scaling laws (SL scaled), as shown in Table 1, which also includes reference motor parameters (FEM ref.) used in the analyses. Figures 6 and 7 show the magnetic flux density distributions in the reference motor and scaled motor respectively under open-circuit conditions, while Figures 8 and 9 represent steady-state operation at rated conditions.

Table 1: Comparison of the referent motor obtained with FEM (FEM ref.) and scaled motor obtained with FEM (FEM scaled) and with scaling laws (SL scaled). Source: Author.

Parameter	FEM ref.	FEM scaled	SL scaled	% diff
slots	48	48	48	0
Nc	9	9	9	0
ap	1	1	1	0
Dso	269,24	134,62	134,62	0
Dsi	161,9	80,95	80,95	0
hs0	1,02	0,51	0,51	0
hs2	29,5	14,75	14,75	0
bs0	1,93	0,965	0,965	0
bs1	5	2,5	2,5	0
bs2	8	4	4	0
Aslot	216,88	54,22	54,22	0
poles	8	8	8	0
Dro	160,4	80,2	80,2	0
Dri	110,64	55,32	55,32	0
D1	157,44	78,72	78,72	0
O1	3	1,5	1,5	0
O2	7,28	3,64	3,64	0
B1	4,7	2,35	2,35	0
WRib	14	7	7	0
HRib	3	1,5	1,5	0
DminMag	4,5	2,25	2,25	0
Mthick	6,48	3,24	3,24	0
Mwidth	32	16	16	0
Lstk	83,82	41,91	41,91	0
J	25,7288	205,83	205,83	0
Iph	214,3133	857,2532	857,25	0
Vph	169,7192	5,1446133	5,30	0,03
VLL	293,9623	7,9920994	9,18	0,13
Rph	50,61	1,5815625	1,58	0
Omega	1200	1200	1200	0
Teixo	397,88	38,7933	49,73	0,22
Tem	401,3348	47,658508	50,16	0,05
Peixo	50	4,875	6,25	0,22
Pem	50,433218	5,9889447	6,30	0,05
Pin	65,7907	6,7435468	8,22	0,18
PCu	14740,161	7296,3797	7370,08	0,01
PFe	192,4496	4,570678	24,05	0,81
eff	76,43	81,340661	84,72	0,04
Bmax	2,25	2,26	-	0

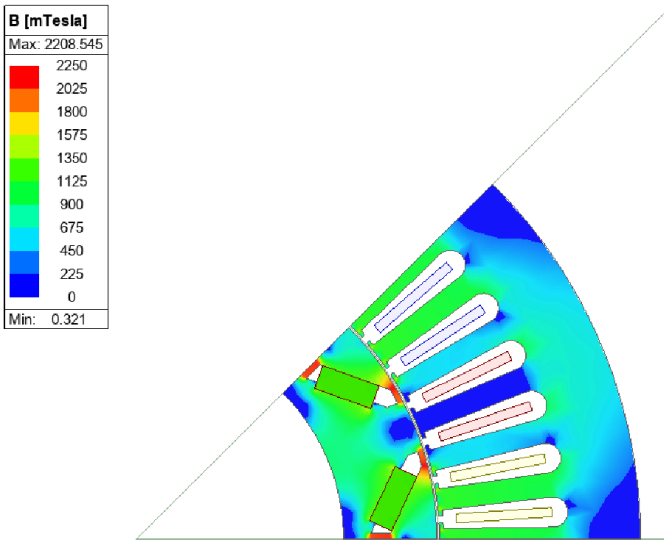

Figure 6: Flux density distribution of the referent machine in open circuit condition. Source: Author.

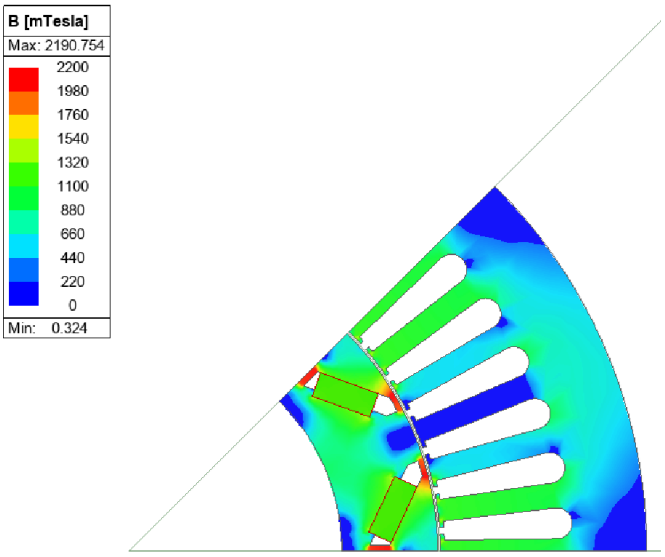

Figure 7: Flux density distribution of the scaled motor in open circuit condition. Source: Author.

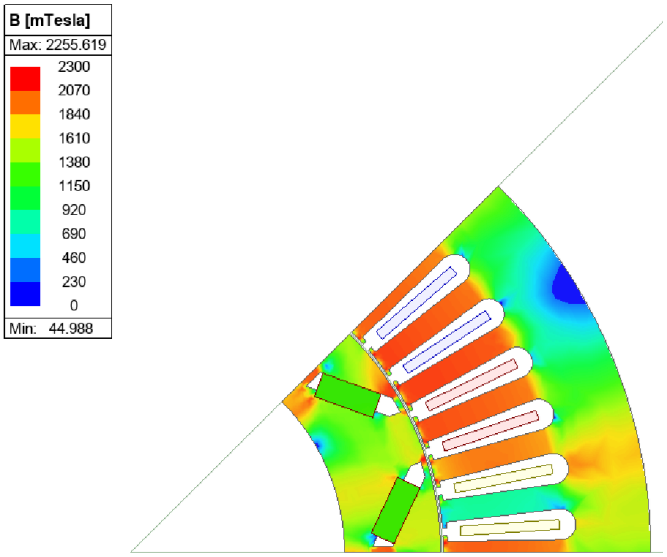

Figure 8: Flux density distribution of the referent motor in rated condition. Source: Author

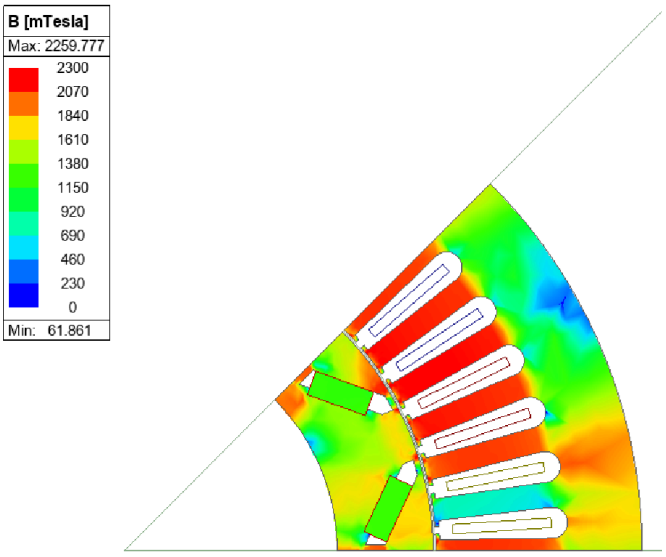

Figure 9: Flux density distribution of the scaled motor in rated condition. Source: Author.

Key parameters for analysis of the scaled motor were obtained with a maximum percentage difference of 22%. The largest differences were found in parameters that neglected end winding influences, such as the d and q inductances and flux linkages, which were used to calculate the electromagnetic torque. The end winding influence is mostly affected by radial scaling, due to the change in the geometry cross-section (Stipetic et al., 2016)

It can be observed that the magnetic flux density distributions are similar, with close maximum and minimum values, as expected based on the considerations made when applying the scaling factors.

CONCLUSION

This study successfully achieved its objective of developing and presenting design methodology based on scaling laws PMaSyRM motors, demonstrating a maximum 22% parameter deviation between scaled and FEM-calculated values while maintaining magnetic flux density distributions. The three-stage approach (reference motor FEM analysis → scale factor determination → scaled parameter calculation) proved effective for rapid motor prototyping, particularly when using the 2004 Toyota Prius motor as a reference platform.

For future studies, an optimization process integration can be explored, in which scaling laws are implemented in an interactive optimization routine where multiple designs are evaluated for achieving a target torque-speed-efficiency map. This integration can accelerate development of EV traction motors with rare-earth magnets usage being minimized with the usage of a PMaSyRM topology. The scaling law approach presents significant time savings in early-stage motor design while maintaining acceptable accuracy, allowing for

further investigation into multi-objective optimization frameworks and expanded material compatibility studies.

ACKNOWLEDGMENTS

This work was conducted with scholarships and financial support from Research Development Foundation - FUNDEP Rota 2030/Line V, from São Paulo Research Foundation - FAPESP (grant 2021/14026-8), from Brazilian National Council for Scientific and Technological Development - CNPq (308389/2022-0), Incentive Program for New Professors at Unicamp - PIND (2500/23) and the Universidade Estadual de Campinas (UNICAMP).

REFERENCES

[1] CANDELO ZULUAGA, Carlos Andres. Design optimization and performance analysis methodology for PMSMs to improve efficiency in hydraulic applications. 2022.

[2] PYRHONEN, Juha; JOKINEN, Tapani; HRABOVCOVA, Valeria. Design of rotating electrical machines. John Wiley & Sons, 2013.

[3] HANSELMAN, Duane C. Brushless permanent magnet motor design. The Writers' Collective, 2003.

[4] BEM, Guilherme Consul Soares de. Análise e simulação de motores síncronos de ímãs permanentes para uso automotivo. 2021.

[5] RUWER, Sherfis Gibran. Projeto eletromagnético de um motor síncrono com ímãs permanentes para aplicação espacial em rodas de reação de satélites. sl] Instituto Nacional de Pesquisas Espaciais, 2015.

[6] LIU, Jinhai; CHEN, Wei. Generalized DQ model of the permanent magnet synchronous motor based on extended park transformation. In: 2013 1st International Future Energy Electronics Conference (IFEEC). IEEE, 2013. p. 885-890.

[7] CELIK, Senol. The effects of climate change on human behaviors. In: Environment, climate, plant and vegetation growth. Cham: Springer International Publishing, 2020. p. 577-589.

[8] HUANG, Yuhan et al. A review of strategies for mitigating roadside air pollution in urban street canyons. Environmental Pollution, v. 280, p. 116971, 2021.

[9] LOGANAYAKI, A.; KUMAR, R. Bharani. Permanent magnet synchronous motor for electric vehicle applications. In: 2019 5th international conference on advanced computing & communication systems (ICACCS). IEEE, 2019. p. 1064-1069.

[10] MILLER, Josh; DU, Li; KODJAK, Drew. Impacts of world-class vehicle efficiency and emissions regulations in select G20 countries. ICCT: Washington, DC, USA, v. 24, 2017.

[11] STIPETIC, Stjepan; ZARKO, Damir; POPESCU, Mircea. Ultra‐fast axial and radial scaling of synchronous permanent magnet machines. IET Electric Power Applications, v. 10, n. 7, p. 658-666, 2016.

[12] STIPETIC, Stjepan; ZARKO, Damir; POPESCU, Mircea. Scaling laws for synchronous permanent magnet machines. In: 2015 Tenth International Conference on Ecological Vehicles and Renewable Energies (EVER). IEEE, 2015. p. 1-7.

[13] AYERS, C. W. Evaluation of 2004 Toyota Prius hybrid electric drive system interim report. Oak Ridge National Lab.(ORNL), Oak Ridge, TN (United States), 2004.

[14] HSU, J. S. Report on Toyota/Prius motor design and manufacturing assessment. Oak Ridge National Lab.(ORNL), Oak Ridge, TN (United States), 2004.

[15] HSU, J. S. Report on Toyota/Prius motor torque-capability, torque-property, no-load back EMF, and mechanical losses. Oak Ridge National Lab.(ORNL), Oak Ridge, TN (United States), 2004.